

Tunable magnetic properties in van der Waals crystals $(\text{Fe}_{1-x}\text{Co}_x)_5\text{GeTe}_2$

Congkuan Tian, Feihao Pan, Sheng Xu, Kun Ai, Tianlong Xia, and Peng Cheng*

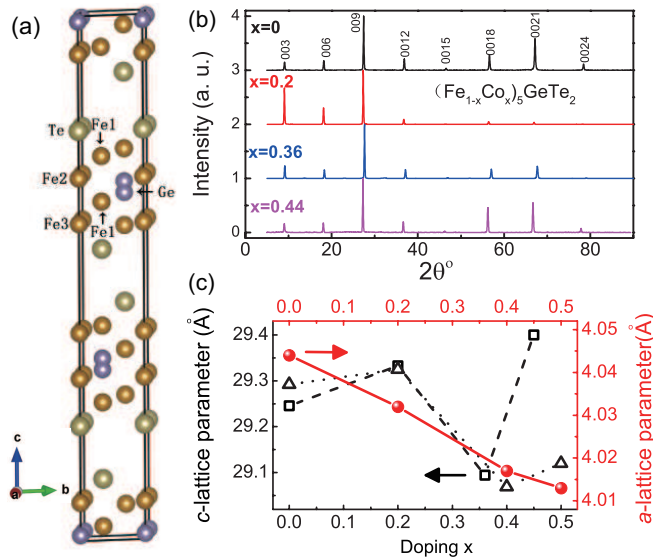
Department of Physics and Beijing Key Laboratory of Opto-electronic Functional Materials & Micro-nano Devices, Renmin University of China, Beijing 100872, P. R. China

(Dated: December 23, 2021)

We report the doping effects of cobalt on van der Waals (vdW) magnet Fe_5GeTe_2 . A series of $(\text{Fe}_{1-x}\text{Co}_x)_5\text{GeTe}_2$ ($0 \leq x \leq 0.44$) single crystals have been successfully grown, their structural, magnetic and transport properties are investigated. For $x=0.20$, The Curie temperature T_C increases from 276 K to 337 K. Moreover, the magnetic easy-axis is reoriented to the ab -plane from the c -axis in undoped Fe_5GeTe_2 with largely enhanced magnetic anisotropy. These magnetic properties would make $(\text{Fe}_{0.8}\text{Co}_{0.2})_5\text{GeTe}_2$ more effective in stabilizing magnetic order in the two-dimensional limit. A complex magnetic phase diagram is identified on the higher doping side. The $x=0.44$ crystal first orders ferromagnetically at $T_C=363$ K then undergoes an antiferromagnetic transition at $T_N=335$ K. Furthermore magnetic-field-induced spin-flop transitions are observed for the AFM ground state. Our work reveals $(\text{Fe}_{1-x}\text{Co}_x)_5\text{GeTe}_2$ as promising candidates for developing new spin-related applications and proposes a method to engineer the magnetic properties of vdW magnet.

The discovery of gate-tunable room-temperature ferromagnetism in two-dimensional (2D) van der Waals (vdW) metal Fe_3GeTe_2 (FGT) has drawn a great deal of attention[1, 2]. FGT has presented plenty of novel properties which may favor applications in spintronic and other technologies such as current-driven magnetization switching[3, 4], tunneling magnetoresistance[5], large anomalous Hall effect[6] and magnetic skyrmions[7]. Recently an analog compound Fe_5GeTe_2 was reported with ferromagnetic (FM) behavior in both bulk crystals and exfoliated thin flakes[8, 9]. Comparing with FGT, bulk Fe_5GeTe_2 crystal has higher Curie temperature T_C but very small magnetic anisotropy[9, 10]. On the other hand, it also exhibits a magnetoelastic coupled first-order transition below 120 K[9]. For potential 2D magnetic materials, strong magnetocrystalline anisotropy and high Curie temperature are both crucial in stabilizing the long-range FM order in monolayer-samples and developing spintronic devices[1, 11]. Therefore it would be important to check whether improved magnetic properties of Fe_5GeTe_2 could be obtained via chemical substitution, which has been proved to be an effective way to manipulate magnetization in ferromagnets[8, 11–14].

In this letter, we report the successful growth and physical properties of $(\text{Fe}_{1-x}\text{Co}_x)_5\text{GeTe}_2$ ($0 \leq x \leq 0.44$) bulk single crystals. Comparing with undoped sample, 20% of Co doping could enhance both the Curie temperature T_C and magnetic anisotropy. On the higher doping side, new antiferromagnetic (AFM) ground states and magnetic field induced spin-flop transitions are observed. These findings suggest Co-doped Fe_5GeTe_2 single crystals could have promising applications in spintronic devices.



*Electronic address: pcheng@ruc.edu.cn

FIG. 1: (a) Crystal structure of Fe_5GeTe_2 with one unit cell is shown and outlined. (b) The XRD patterns of typical $(\text{Fe}_{1-x}\text{Co}_x)_5\text{GeTe}_2$ single crystals at room temperature. (c) Doping dependent lattice parameters for $(\text{Fe}_{1-x}\text{Co}_x)_5\text{GeTe}_2$ at room temperature. Solid spheres and open triangular symbols represent the polycrystalline data. Open squares represent the single-crystal data.

Single crystals of $(\text{Fe}_{1-x}\text{Co}_x)_5\text{GeTe}_2$ were grown by the chemical vapor transport (CVT) method with iodine as the transport agent, similar as growing FGT in previous work[13]. The crystals are flat with typical dimensions of 3 mm×4 mm×0.1 mm and maximum doping up to $x=0.44$. Attempts of crystal growth for higher Co composition were unsuccessful. For single-crystal samples, x represents actual doping levels determined via energy dispersive x-ray spectroscopy (EDS, Oxford X-Max 50). Some polycrystalline samples of $(\text{Fe}_{1-x}\text{Co}_x)_5\text{GeTe}_2$ were synthesized by solid-state reaction method for x-ray diffraction (XRD) studies to check the doping evolution of a -lattice constants. The XRD patterns of all samples were collected from a Bruker D8 Advance x-ray diffractometer using $\text{Cu K}\alpha$ radiation. The magnetization measurements were performed using a Quantum Design MPMS3 and resistivity measurements were carried out on a Quantum Design physical property measurement system (QD PPMS-14T).

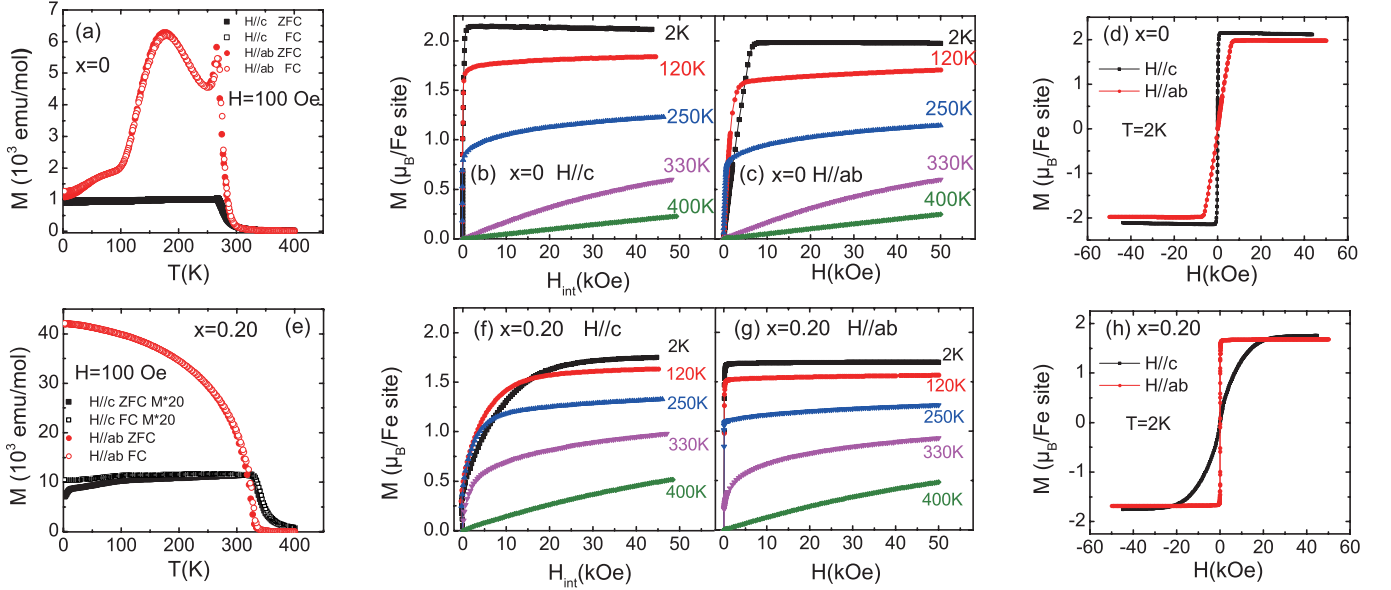


FIG. 2: Anisotropic magnetization data for $x=0$ [(a)-(d)] and $x=0.20$ [(e)-(h)] single crystals respectively. Temperature-dependent magnetization for fixed applied field are shown in (a) and (e), isothermal magnetization curves are shown in (b), (c), (f) and (g), magnetization hysteresis loops at 2 K are presented in (d) and (h).

As shown in Fig. 1(a), the structure of Fe_5GeTe_2 is made up of 2D slabs of Fe and Ge between layers of Te. The vdW gap between Te layers makes crystals cleavable. All the XRD patterns of our $(\text{Fe}_{1-x}\text{Co}_x)_5\text{GeTe}_2$ samples could be described by a rhombohedral $R\bar{3}m$ structure as in previous report[9, 10]. This crystal structure contains three different Fe positions per unit cell. Based on chemical analysis via EDS, the samples all exhibit some iron deficiency in the range of $0.02 \leq \delta \leq 0.08$. Exactly speaking, the samples should be expressed as $(\text{Fe}_{1-x-\delta}\text{Co}_x)_5\text{GeTe}_2$. Nevertheless we found that the tunable magnetic properties mostly depend on the relative cobalt doping concentration. So a simplified expression $(\text{Fe}_{1-x}\text{Co}_x)_5\text{GeTe}_2$ is used to describe our samples in this work. Fig. 1(b) presents the XRD data of single crystals with $x=0$, $x=0.20$, $x=0.36$ and $x=0.44$ respectively. The peaks can be indexed by $(0\ 0\ 3L)$ with $L = 1, 2, 3 \dots$ and no impurity peaks are found within the instrument resolution. The doping dependent lattice parameters derived from the x-ray data are presented in Fig. 1(c). The a -lattice parameters (solid spheres) decrease monotonically with increasing x while the c -lattice parameters show a nonmonotonical behavior with doping for both polycrystalline samples (open triangular symbols) and single crystals (open squares).

Fig. 2 shows the comparison of DC magnetization for $x=0$ and $x=0.20$ single crystals. For undoped Fe_5GeTe_2 , T_C is determined to be 276 K from the temperature dependent magnetization data (Fig. 2(a)). The soft ferromagnetic properties with low coercive field and the magnetic remanence to saturated magnetization ratio are similar as previous reports[8–10] (Fig. 2(d)). Isothermal magnetization curves (M - H) measured under magnetic field applied either parallel to the c -axis ($H\parallel c$) or to the ab plane ($H\parallel ab$) are shown in Fig. 2(b) and (c). Demagnetization corrections have been applied on the $H\parallel c$ data and H_{int} is the internal field. Similar as previous reports, the magnetic moments prefer to align along the c -axis with an anisotropy field of 0.7 T at 2 K[9, 10]. For $x=0.20$, contrasting magnetic

properties are presented in Fig. 2(e)-(h). First of all, the Curie temperature T_C increases to 337 K. This value is double confirmed from the derivatives of both T -dependent DC (Fig. 2(e)) and AC susceptibilities. This result is quite unusual because typically the introduction of dopant tends to suppress T_C because of impurity-induced disorder effect as in Co-doped Fe_3GeTe_2 [13]. Secondly, the isothermal magnetization and hysteresis loops data show that the magnetic easy-axis of $x=0.20$ crystal is reoriented to the ab -plane in contrast to the c -axis in $x=0$. The easy-axis magnetism of $x=0.20$ has an anisotropy field on the order of 2 T at 2 K which is also much larger than that in $x=0$. Especially at high temperatures such as 120 K and 250 K, when the magnetization of Fe_5GeTe_2 becomes nearly isotropic the $x=0.20$ sample still keeps a large anisotropy field. To sum up, 20% of Co doping could effectively tune the magnetic easy-axis of Fe_5GeTe_2 , both T_C and magnetic anisotropy are significantly enhanced.

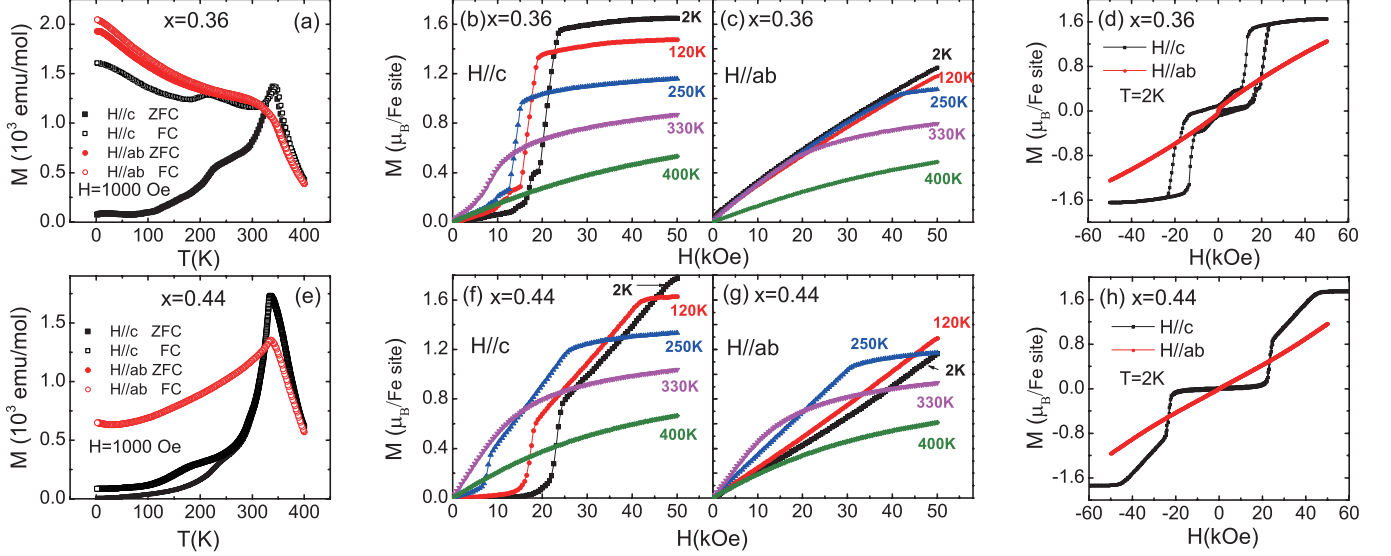


FIG. 3: Anisotropic magnetization data for $x=0.36$ [(a)-(d)] and $x=0.44$ [(e)-(h)] single crystals respectively. Temperature-dependent magnetization for fixed applied field are shown in (a) and (e), isothermal magnetization curves are shown in (b), (c), (f) and (g), magnetization hysteresis loops at 2 K are presented in (d) and (h).

Another feature of $x=0.20$ is the absence of the phase transition near 120 K. Previous neutron diffraction and Mössbauer spectra studies confirm the existence of a first-order magneto-structural transition below 120 K for Fe_5GeTe_2 due to the FM ordering of Fe(1) sites[9]. This phase transition results in kink-features in both M - T curve (Fig. 2(a)) and temperature dependent resistivity data (R - T curve, Fig. 4(a))[10]. However for $x=0.20$, both the kink-features in M - T and R - T curves disappear as shown in Fig. 2(e) and Fig. 4(a), indicating the suppression of this phase transition by Co doping. Since the occupancy rate of Fe(1) is just around 20%[9], it is likely that the dopants mainly occupy the Fe(1) sites thus suppressing the transition. There is also a possibility that the enhanced T_C and magnetic anisotropy are associated with the suppression of this phase transition.

On the higher doping side, $(\text{Fe}_{1-x}\text{Co}_x)_5\text{GeTe}_2$ shows a markedly different magnetic behavior. For $x=0.36$, the peak at $T=340$ K in both zero-field-cooling (ZFC) and field-cooling (FC) M - T curves with $H||c$ suggest the occurrence of an AFM-like transition (Fig. 3(a)). Fig. 3(b) shows the isothermal magnetization data along $H||c$, the virgin magnetization curve of $T=2$ K begins with a gradual increase of the magnetization then a sudden jump at around 2 T, finally approaching the saturation magnetization. This indicates a possible field-induced spin-flop transition from AFM to FM state. The hysteresis loops in Fig. 3(d) suggest the FM state is much weakened but still exists. The $x=0.36$ sample is more like an intermediate phase between FM and AFM region in the phase diagram of $(\text{Fe}_{1-x}\text{Co}_x)_5\text{GeTe}_2$, the magnetization data for $x=0.44$ presented below provide firm evidence for the existence of new AFM and spin-flop transitions.

For $x=0.44$, the ZFC and FC M - T curves along both directions all exhibit sharp peak at $T_N=335$ K and drop rapidly with decreasing temperature (Fig. 3(e)). The peak along $H||c$ is much sharper, indicative of an AFM transition with the magnetic moments being aligned parallel to the c -axis. For the isothermal magnetization and hysteresis loop along $H||c$ below 250 K (Fig. 3(f) and Fig. 3(h)), the initial magnetization shows a very weak linear increase versus field which is consistent with an AFM state. Then at $\mu_0 H \approx 2.3$ T ($T=2$ K), a steep magnetization jump is observed, showing a typical spin-flop transition. In general, the spin-flop transition appears at a critical field H_{SF} and the gain of magnetic energy overcompensates the anisotropy energy required for deviation of spin moments from the preferred orientation[15]. Therefore the anisotropy energy K can be estimated by the equation

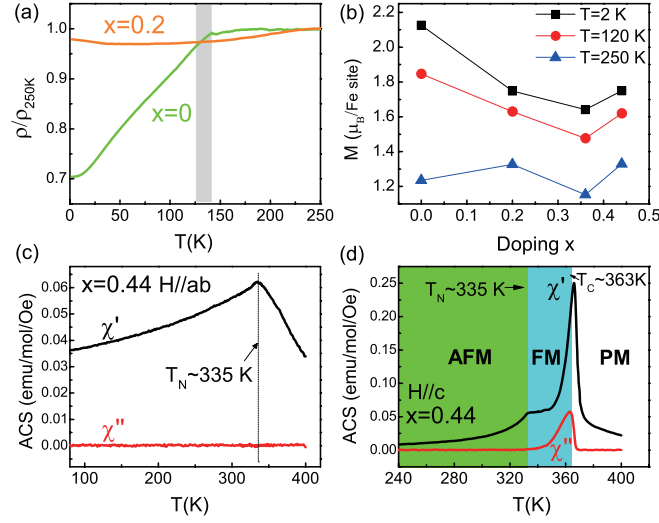


FIG. 4: (a) Temperature dependence of normalized electrical resistivity measured in the ab plane for $x=0$ and $x=0.20$. (b) Doping dependence of saturated magnetic moment per Fe site at 2 K, 120 K and 250 K respectively. The temperature dependent ac susceptibilities of $x=0.44$ crystal measured under oscillated AC field of 2.0 Oe applied along $H||ab$ (c) and $H||c$ directions (d). A phase diagram is superimposed on (d).

$K(T) = 0.5(H_{SF})^2[\chi_{\perp} - \chi_{\parallel}]$ [15], where χ_{\perp} and χ_{\parallel} are the susceptibilities along $H||ab$ and $H||c$ respectively. Our calculations yield an result of $K=1.41 \times 10^6$ ergs/cm³ at $T=2$ K.

The saturated magnetization along $H||c$ occurs at around 5 T indicating the arrival of a complete FM state after the spin-flop transition for $x=0.44$ (Fig. 3(h)). The M-H curves along $H||ab$ show a linear increase as a function of field below 250 K indicating a paramagnetic (PM) response in PM or AFM states (Fig. 3(g)). However the M-H curves above 330 K in both directions exhibit FM-like non-linear behaviors suggest an possible FM order in these temperatures. In order to further elucidate the magnetic states for $x=0.44$, AC susceptibility measurements are carried out under zero DC field and oscillated AC field of 2.0 Oe. The data along $H||ab$ is shown in Fig. 4(c), the peak in real part χ' at 335 K and the absence of any peaks in imaginary part χ'' provide further evidences for the AFM transition. Fig. 4(d) presents the data along $H||c$, a kink in χ' and the absence of any peaks in χ'' at the same $T_N=335$ K are consistent with the AFM transition. Furthermore a notable peak in χ'' at higher temperature $T_C=363$ K is observed. Combining with the rapid increase of magnetization at around 363 K in M-T curves (Fig. 3(e)) and the FM-like non-linear behavior in the M-H curves above 330 K (Fig. 3(f) and (g)), all the experimental observations strongly suggest that there is an FM transition at $T_C=363$ K. So the phase diagram of $x=0.44$ when the magnetic field is not strong enough to cause spin-flop could be drawn in Fig.4 (d). Both DC and AC magnetization data fully support this phase diagram.

The AFM ground state for $x=0.44$ could possibly be associated with the reduction of a -lattice parameter. For one thing, from the FM state in $x=0$ and $x=0.20$ to the AFM state in $x=0.36$ and $x=0.44$, the c -lattice parameters change nonmonotonically. So the change of interlayer distance along c -axis does not seem to be the reason for the occurrence of AFM interactions. For the other, a previous work shows that Ni-doped Fe_5GeTe_2 samples are all ferromagnets with similar c but much larger a parameters comparing with our AFM ordered samples[8]. So the reduced intralayer Fe-Fe distance is likely to make AFM interactions more favorable. As in previous theoretical calculations on CrS_2 and CrI_3 [16, 17], charge carrier doping or doping-induced new stacking orders could also be possible explanations for this tunable magnetism. So our results provide clues and possible methods to manipulate $(\text{Fe}_{1-x}\text{Co}_x)_5\text{GeTe}_2$ few layers transiting between AFM and FM states, which could be employed in future magnetic data recording and information processing. As to the magnetic structure of $x=0.44$, our magnetization data reveal that the magnetic moments tend to align along the c -axis, but could not give whether intralayer or interlayer AFM (as CrI_3 [18]) order is preferred. Further neutron scattering investigations are needed for the final solution. In the development of new spin-related applications, either intrinsic 2D FM or AFM ground state is useful[19, 20]. So $x=0.20$ and $x=0.44$ single crystals could all serve as new vdW candidate magnets for designing nanoscale spintronic devices. Especially the saturated magnetic moments of $(\text{Fe}_{1-x}\text{Co}_x)_5\text{GeTe}_2$ do not have much reduction with increasing x and the values at $T=250$ K are even doping independent as shown in Fig. 4(b). This is also good news for applications.

To summarize our results, we have discovered that the doping of cobalt could significantly tune the bulk magnetic properties of 2D vdW magnets $(\text{Fe}_{1-x}\text{Co}_x)_5\text{GeTe}_2$. For $x=0.20$, both the Curie temperature and the magnetic

anisotropy have increased greatly which makes $(\text{Fe}_{0.8}\text{Co}_{0.2})_5\text{GeTe}_2$ a better potential room-temperature intrinsic 2D magnet comparing with the undoped parent compound. For $x=0.44$, a new AFM ground state with $T_N=335$ K is identified below the FM transition at $T_C=363$ K. Magnetic field induced spin-flop transitions are also observed in this doping range. Our results provide new vdW candidate materials which could potentially be exfoliated for functional vdW heterostructures and devices.

I. ACKNOWLEDGMENTS

The authors thank the helpful discussion with Prof. Wei Ji. This work is supported by the National Natural Science Foundation of China (No. 11227906 and No. 11204373).

-
- [1] Y. Deng, Y. Yu, Y. Song, J. Zhang, N. Z. Wang, Z. Sun, Y. Yi, Y. Z. Wu, S. Wu, J. Zhu, et al., *Nature* **563**, 94 (2018), ISSN 1476-4687, URL <https://doi.org/10.1038/s41586-018-0626-9>.
 - [2] Z. Fei, B. Huang, P. Malinowski, W. Wang, T. Song, J. Sanchez, W. Yao, D. Xiao, X. Zhu, A. F. May, et al., *Nature Materials* **17**, 778 (2018), ISSN 1476-4660, URL <https://doi.org/10.1038/s41563-018-0149-7>.
 - [3] X. Wang, J. Tang, X. Xia, C. He, J. Zhang, Y. Liu, C. Wan, C. Fang, C. Guo, W. Yang, et al., *Science Advances* **5** (2019), <https://advances.sciencemag.org/content/5/8/eaaw8904.full.pdf>, URL <https://advances.sciencemag.org/content/5/8/eaaw8904>.
 - [4] M. Alghamdi, M. Lohmann, J. Li, P. R. Jothi, Q. Shao, M. Aldosary, T. Su, B. P. T. Fokwa, and J. Shi, *Nano Letters* **19**, 4400 (2019), pMID: 31177784, <https://doi.org/10.1021/acs.nanolett.9b01043>, URL <https://doi.org/10.1021/acs.nanolett.9b01043>.
 - [5] Z. Wang, D. Sapkota, T. Taniguchi, K. Watanabe, D. Mandrus, and A. F. Morpurgo, *Nano Letters* **18**, 4303 (2018), pMID: 29870263, <https://doi.org/10.1021/acs.nanolett.8b01278>, URL <https://doi.org/10.1021/acs.nanolett.8b01278>.
 - [6] K. Kim, J. Seo, E. Lee, K.-T. Ko, B. S. Kim, B. G. Jang, J. M. Ok, J. Lee, Y. J. Jo, W. Kang, et al., *Nature Materials* **17**, 794 (2018), ISSN 1476-4660, URL <https://doi.org/10.1038/s41563-018-0132-3>.
 - [7] B. Ding, Z. Li, G. Xu, H. Li, Z. Hou, E. Liu, X. Xi, F. Xu, Y. Yao, and W. Wang, *Nano Letters* **20**, 868 (2020), pMID: 31869236, <https://doi.org/10.1021/acs.nanolett.9b03453>, URL <https://doi.org/10.1021/acs.nanolett.9b03453>.
 - [8] J. Stahl, E. Shlaen, and D. Johrendt, *Z. Anorg. Allg. Chem.* **644**, 1923 (2018), <https://onlinelibrary.wiley.com/doi/pdf/10.1002/zaac.201800456>, URL <https://onlinelibrary.wiley.com/doi/abs/10.1002/zaac.201800456>.
 - [9] A. F. May, D. Ovchinnikov, Q. Zheng, R. Hermann, S. Calder, B. Huang, Z. Fei, Y. Liu, X. Xu, and M. A. McGuire, *ACS Nano* **13**, 4436 (2019), pMID: 30865426, <https://doi.org/10.1021/acs.nano.8b09660>, URL <https://doi.org/10.1021/acs.nano.8b09660>.
 - [10] A. F. May, C. A. Bridges, and M. A. McGuire, *Phys. Rev. Materials* **3**, 104401 (2019), URL <https://link.aps.org/doi/10.1103/PhysRevMaterials.3.104401>.
 - [11] S. Y. Park, D. S. Kim, Y. Liu, J. Hwang, Y. Kim, W. Kim, J.-Y. Kim, C. Petrovic, C. Hwang, S.-K. Mo, et al., *Nano Letters* **20**, 95 (2020), pMID: 31752490, <https://doi.org/10.1021/acs.nanolett.9b03316>, URL <https://doi.org/10.1021/acs.nanolett.9b03316>.
 - [12] G. Drachuck, Z. Salman, M. W. Masters, V. Taufour, T. N. Lamichhane, Q. Lin, W. E. Straszheim, S. L. Bud'ko, and P. C. Canfield, *Phys. Rev. B* **98**, 144434 (2018), URL <https://link.aps.org/doi/10.1103/PhysRevB.98.144434>.
 - [13] C.-K. Tian, C. Wang, W. Ji, J.-C. Wang, T.-L. Xia, L. Wang, J.-J. Liu, H.-X. Zhang, and P. Cheng, *Phys. Rev. B* **99**, 184428 (2019), URL <https://link.aps.org/doi/10.1103/PhysRevB.99.184428>.
 - [14] J. Liu, A. Wang, K. Pu, S. Zhang, J. Yang, T. Musho, and L. Chen, *Phys. Chem. Chem. Phys.* **21**, 7588 (2019), URL <http://dx.doi.org/10.1039/C9CP00151D>.
 - [15] Z. He and Y. Ueda, *Phys. Rev. B* **77**, 052402 (2008), URL <https://link.aps.org/doi/10.1103/PhysRevB.77.052402>.
 - [16] C. Wang, X. Zhou, Y. Pan, J. Qiao, X. Kong, C.-C. Kaun, and W. Ji, *Phys. Rev. B* **97**, 245409 (2018), URL <https://link.aps.org/doi/10.1103/PhysRevB.97.245409>.
 - [17] P. Jiang, C. Wang, D. Chen, Z. Zhong, Z. Yuan, Z.-Y. Lu, and W. Ji, *Phys. Rev. B* **99**, 144401 (2019), URL <https://link.aps.org/doi/10.1103/PhysRevB.99.144401>.
 - [18] B. Huang, G. Clark, E. Navarromoratalla, D. R. Klein, R. Cheng, K. L. Seyler, D. Zhong, E. Schmidgall, M. A. McGuire, and D. H. Cobden, *Nature* **546**, 270 (2017).
 - [19] V. Baltz, A. Manchon, M. Tsoi, T. Moriyama, T. Ono, and Y. Tserkovnyak, *Rev. Mod. Phys.* **90**, 015005 (2018), URL <https://link.aps.org/doi/10.1103/RevModPhys.90.015005>.
 - [20] H. Li, S. Ruan, and Y.-J. Zeng, *Advanced Materials* **31**, 1900065 (2019), <https://onlinelibrary.wiley.com/doi/pdf/10.1002/adma.201900065>, URL <https://onlinelibrary.wiley.com/doi/abs/10.1002/adma.201900065>.